Spring snow albedo feedback over Northern Eurasia:

Comparing in-situ measurements with reanalysis products

Martin **Wegmann**[1], Emanuel **Dutra**[2], Hans-Werner **Jacobi**[1] and Olga **Zolina**[1,3]

[1]*Institute for Geosciences and Environmental Research (IGE), Univ. Grenoble Alpes, CNRS, IRD, Grenoble INP*, Grenoble, France*

** Institute of Engineering Univ. Grenoble Alpes*

[2]*Instituto Dom Luiz, Faculdade de Ciências, Universidade de Lisboa, Lisbon, Portugal*

[3]*Shirshov Institute of Oceanology, Moscow, Russia*

ABSTRACT

This study uses daily observations and modern reanalyses in order to evaluate reanalysis products over Northern Eurasia regarding the spring snow albedo feedback (SAF) during the period from 2000 to 2013. We used the state of the art reanalyses ERA-Interim land and the Modern-Era Retrospective Analysis for Research and Applications Version 2 (MERRA2) as well as an experimental setup of ERA-Interim land with prescribed short grass as land cover to enhance the comparibility with the station data, while underlining the caveats of comparing in-situ observations with gridded data. Snow depth statistics derived from daily station data are well reproduced in all three reanalyses, however day-to-day albedo variability is notably higher in stations compared to any reanalysis product. The ERA-Interim grass setup shows an improved performance in representing albedo variability and generates comparable estimates for the snow albedo in spring. We find that modern reanalyses show a physically consistent representation of SAF, with realistic spatial patterns and area-averaged sensitivity estimates. However, station-based SAF values are significantly higher than in the reanalyses, which is mostly driven by the stronger contrast beween snow and snow-free albedo. Switching to grass-only vegetation in ERA-Interim land increases the SAF values up to the level of station-based estimates. We found no significant trend in the examined 14-year timeseries of SAF, but inter-annual changes of about 0.5% K^{-1} in both station-based and reanalysis estimates were derived. This inter-annual variability is primarily dominated by the variability in the snow melt sensitivity, which is correctly captured in reanalysis products. Although modern reanalyses perform well for snow variables, efforts should be made to improve the representation of dynamic albedo changes.

1. Introduction

Global warming is enhanced at high northern latitudes, where the Arctic near-surface air temperature has risen at twice the rate of the global average in recent decades – a feature called Arctic amplification **(Serreze and Barry 2011).** Climate model experiments for the 21st and 22nd centuries show that Arctic warming will continue and intensify under all emission scenarios (**Collins et al. 2013**). Arctic amplification results from several processes interacting with each other such as the albedo feedback due to a reduction in snow and ice cover, enhanced poleward atmospheric and oceanic heat transport, and changes in humidity **(Serreze and Barry 2011, Pithan and Mauritsen 2014).**

Being one of the critical factors of the Arctic amplification, the surface albedo feedback implies a decrease of reflected shortwave radiation at the top of the atmosphere in conjunction with decreasing surface albedo and increasing near-surface temperature (**Thackeray and Fletcher 2016**). It is considered to be a positive feedback in the sense that an initial warming is strenghtened over time, quantified through the change in surface albedo per unit change of temperature **(Robock 1983, Cess et al. 1991, Qu and Hall 2007)**. Snow melt triggers this feedback via surface absorption of shortwave radiation followed by conversion to longwave radiation, warming the lower layers of the troposphere (**Curry et al. 1996**). Snow albedo feedback (SAF) and its impact on climate have been studied for several decades (**Wexler et al. 1953, Budyko 1969, Schneider and Dickinson 1974, Lian and Cess 1977).** It got further attention in the wake of anthropogenic global warming accompanied by the reduction of snow and ice cover over the Northern Hemisphere (NH) **(Bony et al. 2006, Qu and Hall 2007, Fernandes et al. 2009, Flanner et al. 2011, Qu & Hall 2014, Fletcher et al. 2015, Thackeray and Fletcher 2016).**

During 1979–2011, the Arctic snow cover extent in June decreased at a rate of -21% per decade (**Derksen and Brown 2012**). Climate model projections for the end of the 21st century show an even more reduced Arctic cryosphere and, thus, the SAF will

continue to modulate Arctic warming **(Brutel-Vuilmet et al. 2013).** The SAF is especially effective over the NH since most of it is covered by snow during boreal wintertime **(Groisman et al. 1994). Hall (2004)** found that 50% of the total NH extratropics SAF caused by global warming occurs during spring, while **Qu and Hall (2014)** estimated that the SAF variability between models accounts for 40-50% of the spread in the warming signal over the continents of the NH extratropics.

Several studies investigated spring NH extratropic SAF based on satellite, reanalysis and model datasets **(Fernandes et al. 2009, Fletcher et al. 2012, Qu and Hall 2014, Fletcher et al. 2015).** Satellite-based estimates of SAF vary within ±10% depending on the analysed data set. **Hall et al. (2008)** used the International Satellite Cloud Climatology Project (ISCCP) data (**Schiffer and Rossow 1983**) to calculate a SAF strength of -1.13% K^{-1}, whereas **Fernandes et al. (2009)** using Advanced Very High Resolution Radiometer (AVHRR) data (**Justice et al. 1985**) found a slightly weaker SAF of -0.93% K^{-1}. **Qu and Hall (2014)** determined the SAF using Moderate Resolution Imaging Spectroradiometer (MODIS) data (**Hall et al. 2002**) and found a value of -0.87% K^{-1} for springtime. Considering different spatial and temporal domains as well as the variety of methods applied, the SAF estimates around -1% $K^{-1}$from satellite data can be considered as quantitatively consistent.

Model- and reanalysis-based estimates are somewhat higher compared to those derived from satellite data. **Fletcher et al. (2015)** investigated Coupled Model Intercomparison Project 3 and 5 (CMIP3/CMIP5) ensembles to estimate the SAF for an assortment of Global Climate Models (GCMs). The authors found a SAF ensemble model mean of -1.2% K^{-1} for the NH extratropics, which is in fair agreement with MODIS values, but is higher compared to ISCCP- and AVHHR-based estimates. Within this comparison **Fletcher et al. (2015)** also investigated SAF computations based on ERA-Interim **(Dee et al. 2011),** Modern-Era Retrospective Analysis for Research and Applications (MERRA) **(Rienecker et al. 2011)** and NCEP-2 **(Kanamitsu et al. 2002)** reanalyses, thus, providing the most up to date assessment of SAF in reanalysis datasets. While MERRA data resulted in a slightly weaker SAF of -1.17% K^{-1} compared to ERA-Interim (-1.23% K^{-1}), both reanalyses show similar SAF values compared to MODIS.

That said, most studies use satellite derived albedo data in conjunction with temperature and snow cover data from reanalyses.

Although satellite products of snow cover and albedo cover large parts of the NH, they exhibit low temporal resolution and significant uncertainties for high solar zenith angles as well as complex terrains (eg. **Wang et al. 2014**). **Thackeray and Fletcher (2016)** compared CMIP3/CMIP5 model families and found that the models represent the SAF process rather accurately. However, there are still inherent biases likely related to the use of outdated parameterizations. In this respect the use of in-situ observations would provide an opportunity for evaluating SAF estimates in different gridded datasets and especially among reanalyses. However, estimating SAF in the Arctic using in-situ data is challenging, mostly because of the lack of reliable, relevant observations, both in the temporal and spatial domain. Furthermore, the lack of in-situ SAF estimates hampers the understanding of SAF in high latitude climates (**Graversen and Wang 2009, Gravesen et al. 2014**).

In this study we use a unique dataset of daily observations and modern reanalyses over Northern Eurasia in order (1) to evaluate reanalysis products with respect to radiation and snow properties and (2) to determine the SAF in spring between 2000–2013 based on in-situ measurements. We compare different land-reanalysis products with modified vegetation settings. Specific questions to be addressed in this study are the following: How well do the modern reanalyses reproduce snow and radiation features on a daily resolution? What are realistic estimates of the SAF from the station data over Northern Eurasia and how well do they compare to the gridded reanalyses data? What are the major characteristics of space-time variability of the SAF in station and reanalysis data?

The paper is organized as follows. After describing the different datasets and the methods in sections 2 & 3, we evaluate the daily output for snow, radiation fluxes and temperature within these datasets in section 4.1. In section 4.2 we assess the results of the SAF computations and the differences between products including also an analysis of the spatial and temporal variability. Section 5 discusses the results and considers potential implications for future studies.

2. Data

151 **2.1 Reanalysis Data**

152 To investigate the SAF processes in reanalyses, we evaluated two products: the ERA-
153 Interim-land (ERAI-L, **Balsamo et al. 2015**) and Modern-Era Retrospective analysis
154 for Research and Applications, Version 2 (MERRA2) (**Gelaro et al. 2017**). ERAI-L is
155 a land-surface only simulation driven by the near-surface meteorology and fluxes from
156 the ERA-Interim atmospheric reanalyses (**Dee et al. 2011**). The land-surface model in
157 ERAI-L (HTESSEL) has several enhancements compared with the land-surface model
158 used in ERA-Interim including the snowpack representation (**Dutra et al. 2010**). ERAI-
159 L considers the prognostic evolution of snow mass and density, and for exposed areas
160 there is also a prognostic evolution of snow albedo. For shaded snow, i.e. snow under
161 high vegetation, the albedo is considered constant and dependent on vegetation type
162 (see **Dutra et al. 2010** for more details).
163 MERRA2 also includes a dedicated land module for surface variables. Furthermore, it
164 applies an updated Goddard Earth Observing System (GEOS) model and analysis
165 scheme and assimilates more observations than its predecessor MERRA (**Rienecker et**
166 **al. 2011**). Finally, MERRA2 uses observation-based precipitation data to force its land-
167 surface parameterizations, similar to what formerly was known as MERRA-land.
168 Unlike ERAI-L, MERRA2 consists of a full land-atmosphere reanalysis. Its
169 incremental analysis update (IAU) scheme improves upon 3D-Var by dampening the
170 analysis increment. In IAU, a correction is applied to the forecast model gradually,
171 limiting precipitation spinup in particular.

172 For near-surface temperature we use 2m air temperature for both the reanalyses and
173 observations. Moreover, we do not use albedo computed by the reanalysis, but calculate
174 it from the radiative flux components consistent with the observed albedo. For this
175 purpose, we use upward and downward shortwave radiation at the surface as diagnosed
176 by ERA-Interim and MERRA2 as well as surface net and surface incoming radiation
177 from the station observations. Snow depth is used as inferred by reanalyses and, if
178 needed, converted to cm. More information about general characteristics of reanalysis
179 products in the Arctic can be found in **Lindsay et al. (2014), Dufour et al. (2016)** and
180 **Wegmann et al. (2017).**

181

182

2.1.1 Idealized Reanalysis Experiment

Since the in-situ measurements in this study are observed over clear cut vegetation, idealized simulations prescribing grassland everywhere were carried out with the ERAI-L configuration (hereafter ERA-Interim land grass only (ERAI-LG)). The ERAI-LG simulation was carried out with the same model and setup as ERAI-L, differing only in the land cover used. The land-surface model used in ERAI-L, HTESSEL, accounts for sub-grid scale land cover variability by representing several land tiles, namely: low vegetation, high vegetation, bare ground, exposed snow (snow on top of bare ground or low vegetation), shaded snow (snow under high vegetation) and interception. The land cover is prescribed with four maps: low and high vegetation cover (cvl and cvh) and low and high vegetation types (tvl and tvh). The bare ground fraction is computed as cvb= 1 - cvl - cvh, the snow fraction is a function of the mean grid-box snow depth and the interception fraction as a function of the mean interception reservoir water content. For the ERAI-LG simulation, the high vegetation cover was set to zero (cvh=0), the low vegetation cover to one (cvl=1) and the low vegetation type to grassland. In this idealized simulation the entire globe was covered in grass land so that only the low vegetation and exposed snow (when snow is present) tiles were active. The main goal of this simulation is to evaluate the role of land cover when comparing point observations with gridded reanalysis and to evaluate pathways to improve reananalyses in representing albedo processes.

2.2 Observational in-situ data

To evaluate reanalysis perfomance, we used newly assembled in-situ radiation observations from Russian meterological stations. This dataset includes 4-hourly solar radiation and radiation balance data from the World Meteorological Organisation (WMO) World Radiation Network of the World Radiation Data Center (WRDC) at the Voeikov Main Geophysical Observatory, Saint Petersburg, Russia. The original WRDC data contains time series from 65 locations. We selected 47 stations for this study because they overlap with daily snow depth and 2m temperature observations (see Supplement Table 1). Of these 47 stations three were attributed by ERAI-L to

ocean gridpoints and we decided to remove the three coastal stations from the initial dataset, so that the final dataset consists of 44 stations. Temperature and snow depth observations were taken from the All-Russian Research Institute of Hydrometeorological Information World Data Centre (RIHMI-WDC), Obninsk, Russia. A detailed description of this dataset is provided by **Bulygina et al. (2010)**. This dataset includes snow depth as well as snow cover fraction around meteorological stations. Snow cover information in this data set is not stored in percentages, but rather in a scale of integers from 0 to 10 (for example, 50% is assigned a value of 5, but so is 53%). This makes these data hardly applicable for precise SAF calculations. Snow depth information is measured in centimeters with the precision of 1 cm. This might lead to an underestimation of snow depth in case of shallow snow (between 0 and 1 cm). All variables (temperature, snow depth and snow cover, surface LW radiation budget and surface SW radiation, the sum of the surface short-wave and long-wave radiation budgets) were represented as daily time series for the period 2000–2013, which is the time period available for the radiation observations by the Voeikov Main Geophysical Observatory.

Figure 1 shows the location of the stations together with the climatological 2000–2013 MAMJ snow depth as computed by ERAI-L. The distribution of stations is quite heterogeneous, with very few stations located in Eastern Siberia and in the Far East. Moreover, some stations have prolonged periods of missing values; six stations have more than 50% missing values in the daily timeseries for MAMJ. For monthly means, the total number of missing values generally decreases from 2000 to 2013 (see Supplementary Figure 1). However, data for the year 2009 are missing at 44 out of 47 stations during MAM period and at 3 stations in June. Nevertheless, spatial and temporal coverage of this data set is exceptional for the analysis of albedo in this region. It is also important to note that neither snow nor radiation from these stations were assimilated in the reanalysis datasets and, therefore, our inter-comparisons are completely independent.

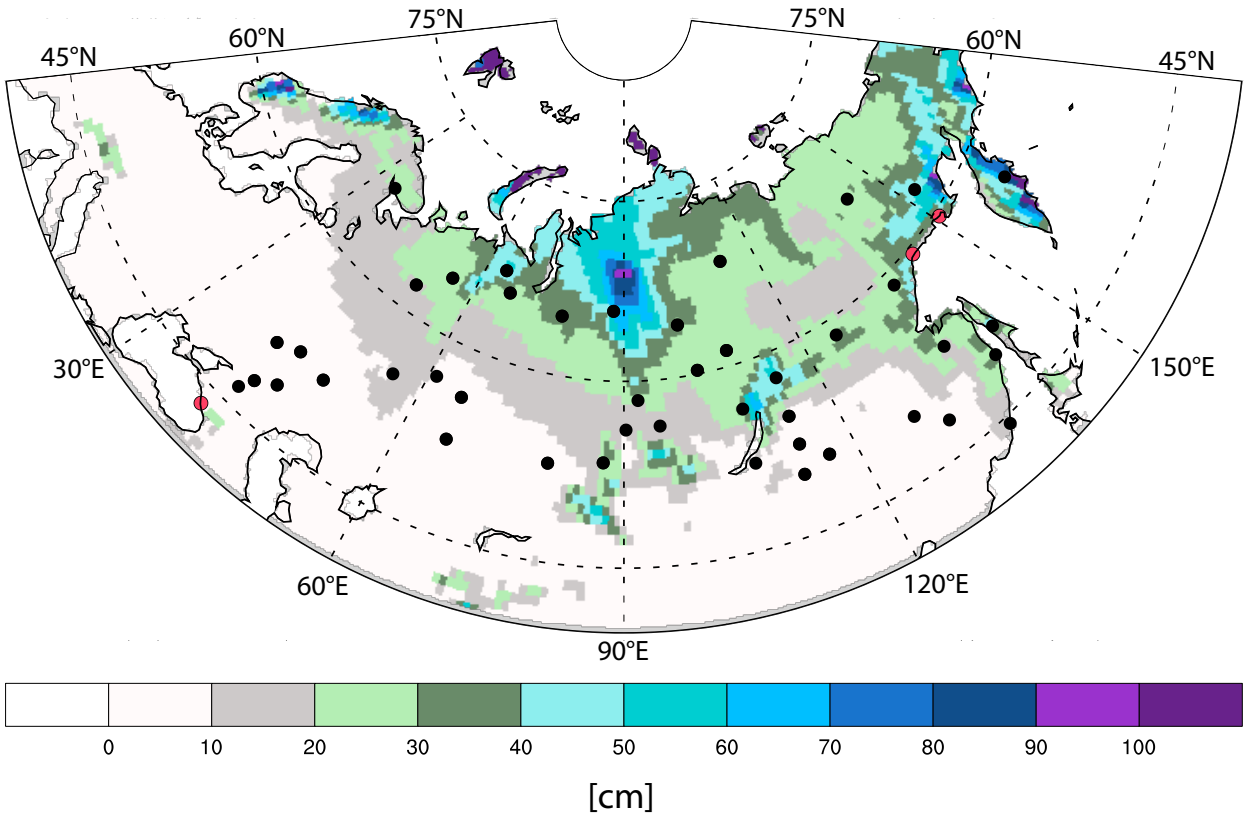

Figure 1: Station location and snowdepth [cm] for the 2000–2013 MAMJ average taken from ERAI-L. Red colored stations are excluded by the land-sea mask of ERAI-L.

3. Methods

To evaluate the climatic variables needed for the SAF computation, we first compared daily values of snow depth, albedo and 2m temperature from the meteorological stations with those from the reanalyses. To co-locate observations with reanalyses, we extracted the information of the gridcell from the reanalysis, in which the station is located. In case of ERA-Interim land, horizontal resolution is 0.75° x 0.75° degrees, whereas MERRA2 has a horizontal resolution of 0.5° x 0.625° degrees. That said, the extracted values of the gridcell are expected show less variability and lower peak values, since they are integrated over a larger spatial domain, which dampens extreme values. We then derived long-term differences, performed a correlation analysis and also compared the variability among the datasets for the MAMJ period.

Since the SAF signals for the seasonal cycle and under long-term climate change are highly correlated **(Hall and Qu 2006)**, we focus here on the evaluation of the seasonal cycle. Snow cover is converted from snow depth following a logarithmic equation

according to which 2.5 cm of snow depth was defined as equivalent to 100% snow cover (**Fletcher et al. 2015)**. We split SAF into a snow cover component (SNC) and a temperature/metamorphosis component (TEM). SNC relates to the decrease of the albedo linked to the earlier melting of snow. TEM concerns the reduction of snow albedo due to enhanced metamorphism and larger grain sizes at warmer temperatures. In this study we focus on these two components of the feedback process, rather than the general classic term for net SAF ($\Delta\boldsymbol{\alpha}/\Delta\boldsymbol{T}$), since our goal is to evaluate differences in the more intricate terms of SAF. In the following, we assume that SAF=SNC+TEM, which was shown to be true in nearly all cases for the NH (**Fletcher et al. 2012, Fletcher et al. 2015**). Therefore, we compute the two terms as

$$\boldsymbol{SNC} = (\overline{\boldsymbol{\alpha_{snow}}} - \boldsymbol{\alpha_{land}})\,\Delta\boldsymbol{S_c}/\Delta\boldsymbol{T_{2m}} \quad \textbf{(1)}$$

and

$$\boldsymbol{TEM} = \overline{\boldsymbol{S_c}}\,\Delta\boldsymbol{\alpha_{snow}}/\Delta\boldsymbol{T_{2m}}\ , \quad \textbf{(2)}$$

where $\boldsymbol{\alpha_{snow}}$ is the snow-covered surface albedo, $\boldsymbol{\alpha_{land}}$ is the snow-free surface albedo, $\boldsymbol{S_c}$ is the snow cover fraction and $\boldsymbol{T_{2m}}$ is the 2 m temperature. The first term of SNC ($\overline{\boldsymbol{\alpha_{snow}}} - \boldsymbol{\alpha_{land}}$) is also known as albedo contrast, whereas the second term ($\Delta\boldsymbol{S_c}/\Delta\boldsymbol{T_{2m}}$) will be referred to as snow melt sensitivity. In (1) and (2) deltas indicate month-to-month changes and the overbars indicate means over the two adjacent months. Note that $\Delta\boldsymbol{T_{2m}}$ does not represent a hemispheric mean but rather the difference at an individual location. It was found that the contribution of SNC and TEM to the overall SAF is between 60 to 70% and 30 to 40 % for the NH (**Fletcher et al. 2015**).

In our SAF assessment, we use 2 m temperature as a surrogate for near surface air temperaure, since the latter variable is not represented by stations. Using 2m temperature introduces some uncertainty to the results since atmospheric temperature advection can play a role in local temperature evolution. However, by now multiple studies (**Fletcher et al. 2015, Xiao et al. 2017, Kevin et al. 2017**) deal with 2 m temperature in their SAF assessment, mainly also due to the same comparability issues.

Since daily data are available, we define $\boldsymbol{\alpha_{snow}}$ as the monthly mean over all daily estimates during the specific month when $\boldsymbol{S_c} = \mathbf{100\%}$**.** Moreover, we define $\boldsymbol{\alpha_{land}}$ as the mean over all daily estimates during MAMJ (in some stations this might only occur

291 in June) when $\boldsymbol{S_c = 0\%}$. This allows for a less artifical estimation of $\boldsymbol{\alpha_{land}}$ than
292 conventionally using summer (e.g. August) albedo.

293

294 **4 Results**

295 **4.1 Daily data evaluation**

296 Since 2m air temperature in reanalyses has been comprehensively evaluated in previous
297 studies (eg. **Schubert et al. 2014, Lindsay et al. 2014**), we only perform a general
298 comparative asssement of the daily values of albedo and snow depth in the SAF
299 computations. That said, **Lindsay et. al 2014** found that 2m temperatures show slight
300 negative biases over Russia in Winter for both ERA-Interim and MERRA1, whereas in
301 summer ERA-Interim shows basically no bias and MERRA1 shows slight positive
302 biases. Improvements in this regard from MERRA1 to MERRA2 are to be expected.

303 Figure 2 shows an overall comparison between station data and reanalyses in terms of
304 correlations, differences and magnitude of variability quantified by the standard
305 deviation for the albedo and snow depths. On a day-to-day basis MERRA2 and ERAI-
306 L are underestimating average albedo values compared to observations by about 0.1
307 during MAMJ (Figure 2a). On the other hand, ERAI-LG shows a much smaller average
308 deviation from the station data with differences close to zero. However, the overall
309 range of the boxplot for ERAI-LG is similar to the other two reanalyses resulting in
310 only slightly less absolute deviations from the observations.

311 For snow depth (Figure 2b), all three reanalysis datasets show an overestimation of
312 daily values for MAMJ. Interestingly, ERAI-LG shows the largest deviations from
313 observed values, although the grass better represents the conditions at the observational
314 sites. This can be caused by biases in the observations due to surrounding higher
315 vegetation creating a snowfall shadow or negative instrumental biases (**Rasmussen et**
316 **al. 2012**). Moreover, positive biases in particular for precipitation can occur in
317 reanalysis products (**Brun et al. 2013**).

318 The analysis of daily correlations (Figure 2 c and d) demonstrates that the correlations
319 for the albedo are generally low among all three experiments, whereas for some stations
320 they can reach correlation coefficients higher than 0.8. Surprisingly, the correlations

between MERRA2 and station data are the highest for albedo and the lowest for snow depth. The observed difference between MERRA2 and the ECMWF experiments regarding the correlation for albedo can likely be explained by the introduction of aerosols (and their respective deposition) in MERRA2 (see the Supplement for a initial investigation). For snow depth, the correlation values are dominated by snowfall and melting events. Also in this case, the grass-only experiment shows no increased performance compared to the classic ERAI setup.

All reanalyses severely underestimate the day-to-day variability of the albedo (Figure 2 e and f). MERRA2 and ERAI-L show similar means, but reach the overall station level only in specific grid cells. A clear improvement is observed in ERAI-LG, which shows the smallest deviation from station estimates. Nevertheless, all modern reanalyses fail to adequately reproduce daily varability in the observed albedo. On the other hand, for snow depth the agreement is very good. The means of all four products are around the values of 8 to 10 cm, with the grass-only experiment being the closest to the average station variability.

In summary, the boxplot analysis (Figures 2) reveals that there is a general improvement in agreement between stations and ERAI-L if vegetation is set to grass only. However, none of the reanalysis products can accurately reproduce day-to-day albedo variability. This is likely explained by the comparison of grid versus point observations, where small-scale variations are averaged out.

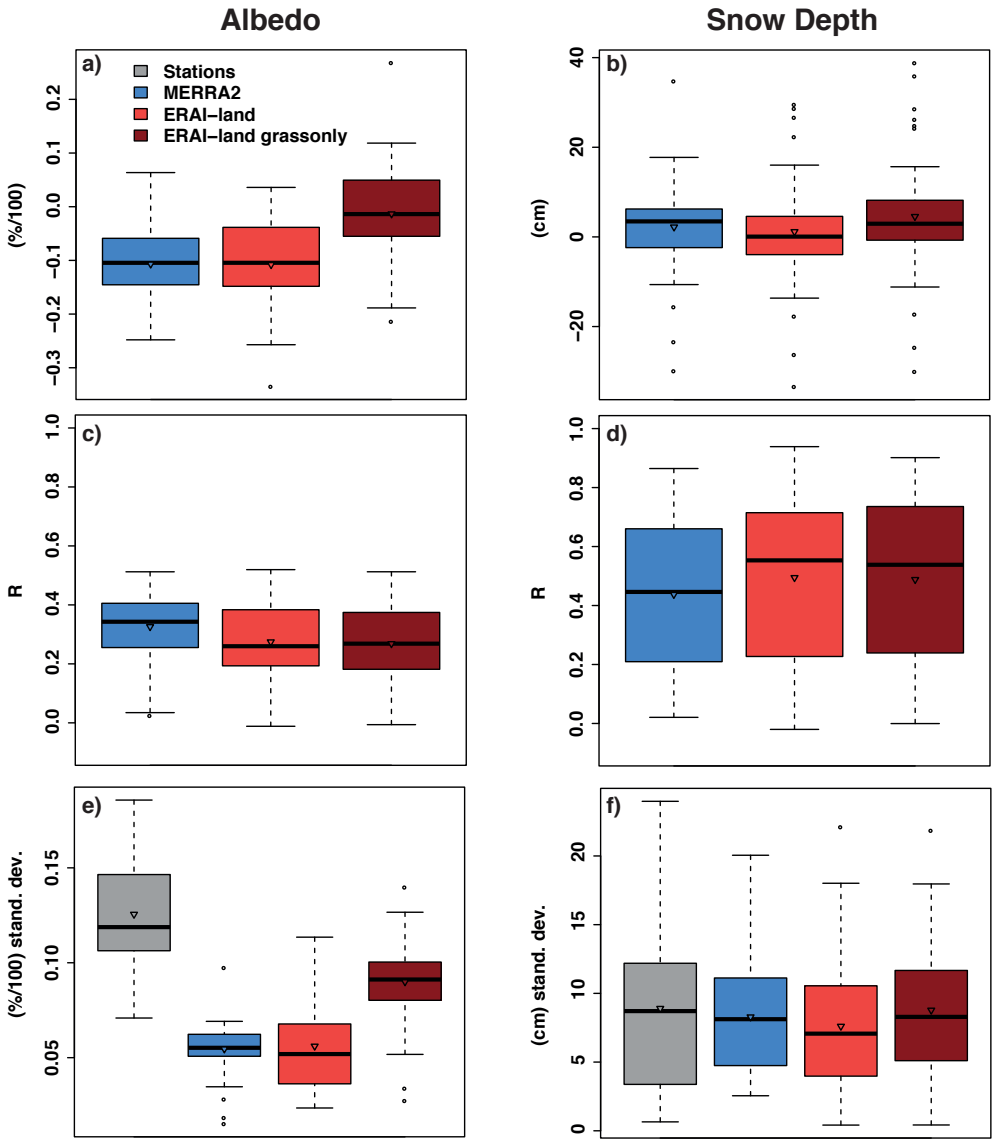

341

342 **Figure 2: Boxplot analysis for daily albedo (a, c, e) and snow depth (b, d, f)**
343 **estimates using data from 44 locations over 2000–2013 MAMJ period. (a) and (b)**
344 **Difference between station and reanalysis, (c) and (d) linear correlation between**
345 **station and reanalysis, (e) and (f) standard deviation. Triangle indicates the mean**
346 **value.**

347

348

349

350

4.2 Analysis of feedback components

To assess regional patterns of key SAF components, we show their spatial distribution over Russia as revealed by the observations in Figure 3 (See Supplement Figures 2-4 for the respective distribution from the reanalyses data).

Strong SNC (Figure 3a) responses in the station data are observed in Southern European Russia and Western Siberia as well as over the Far East. The weaker responses are observed in Southern Eastern Siberia. TEM (Figure 3b) follows a similar distribution but is more homogeneously distributed with most negative values in Central Siberia and towards the Arctic coastline. Snow melt sensitivity (Figure 3c) is strongest in the mid-latitudinal and subpolar regions north of 50° N, such as Finland to the southeast, west and north of Lake Baikal and along the Pacific Coast. Here the temperatures react most strongly to seasonal snow melt. While there is a broad agreement between the stations and ERAI-LG in this region, stations show a somewhat stronger snow melt sensitvity (not shown). Snow melt sensitvity is a key factor for the SNC calculations and, thus, shapes the spatial variability of SNC.

The other key factor in the SNC calculations is the contrast in albedo between snow-covered and snow-free periods (Figure 3d). The observed albedo contrast is characterized by a relatively homogeneous patttern with somewhat smaller values in the southern regions, especially over Southern Eastern Siberia east of the Lake Baikal. In general, a north-south gradient is visible with similar patterns as in SNC. Mean albedo for spring (Figure 3e) shows that highest values are found closer to the Arctic coastline, in Central Siberia and towards the western border. Lower mean albedo values are mostly located east of Lake Baikal. This distribution is in general agreement with the reanalyses datasets, especially for the lower values in the south east.

Finally, since TEM follows closely the general MAMJ snow distribution, we show average snow depth in Figure 3f. A clear north-south gradient is visible with hotspots at the Pacific coast and towards the Barents-Kara sea. Moreover, snow depths from stations follow closely the ERA-L snowdepth distribution shown in Figure 1.

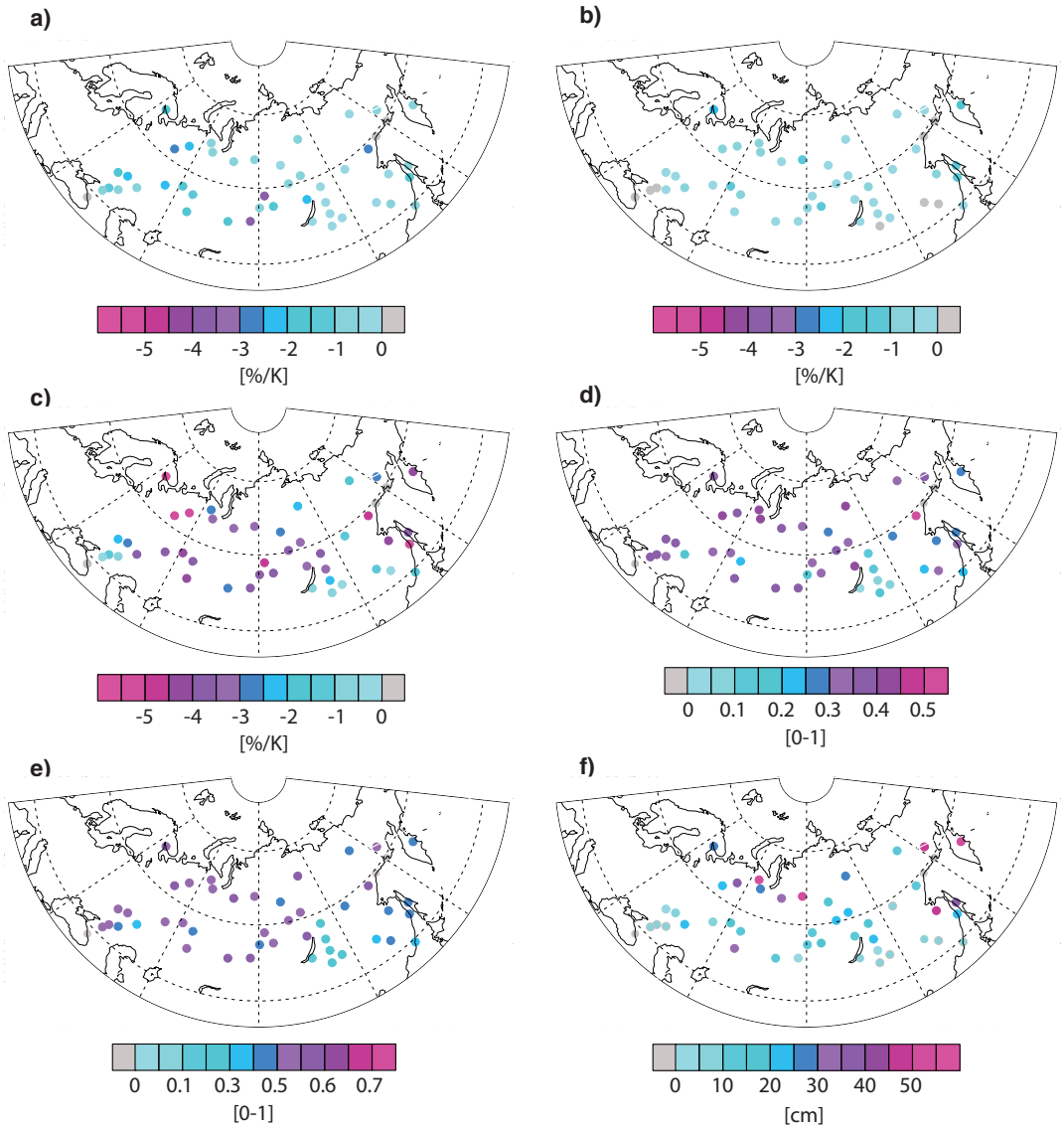

379

380 **Figure 3: Mean SAF components in station data for 2000–2013 MAMJ. a) SNC,**
381 **b) TEM, c) snow melt sensitivity, d) mean albedo contrast, e) mean albedo, f) snow**
382 **depth.**

383

384 To analyse the differences between the datasets and to put the station data in context,
385 Figure 4a shows the response for SAF computed for the entire period 2000-2013 and
386 all 44 locations. Stations show much stronger SAF (-2.5% K^{-1}) compared to MERRA
387 (-1.6% K^{-1}) and ERAI-L (-1.8% K^{-1}). At the same time ERAI-LG shows SAF estimate
388 close to that derived from the station data (-2.8% K^{-1}). Thus, changing the vegetation
389 to short grass adds an additional 1% albedo decrease per degree of warming to the
390 feedback process. The further analysis of the two components of SAF (SNC and TEM,

391 Figure 4 b and c) shows that ERAI-LG reproduces well the SNC signal derived from
392 the station data (-1.6% K^{-1} mean for stations and -1.7% K^{-1} mean for ERAI-LG),
393 whereas the other two reanalyses show much weaker SNC values. The lowest value of
394 -0.56% K^{-1} was obtained from the MERRA2 data. In general, SNC responses largely
395 explain differences in SAF (Figure 4a).

396 For TEM values (Figure 4c), all three reanalyses are in a good agreement with the
397 observations with MERRA2 showing the best agreement. Changing the vegetation to
398 grass in ERA-Interim results in a TEM component, which is 0.4-0.5% K^{-1} stronger
399 compared to the standard version of ERA-Interim. Given that TEM represents the
400 response to snow metamorphosis, good performance of MERRA2 is in agreement with
401 findings implied by Figure 2. However it is worth noting that for the station network as
402 well as for the ECMWF experiments, locations with positive TEM are calculated. This
403 is due to snow albedo changes being positive in some instances (Figure 4c).

404 To further investigate the nature of the SNC and TEM responses we show in Figure 4d
405 the results for snow melt sensitivity, which is one of the two key components in the
406 SNC response (1). This component is barely influenced by the underlying vegetation.
407 All three reanalysis datasets agree very well with the station network, with ERAI-LG
408 showing the closest agreement for both mean and median. This indicates an accurate
409 representation of this relationship in both NASA and ECMWF land surface modules.

410 Figure 4d implies that the changes in the SNC should stem from the albedo contrast,
411 the second key component expressed as the average difference between albedo values
412 for a complete snowcover and snow-free conditions (Figure 4e). Indeed, MERRA2
413 shows the lowest albedo contrast among all datasets, resulting in very low SNC values.
414 Albedo contrast in ERAI-L is higher than MERRA2, but is on average still lower
415 compared to the observations, which show average values around 0.35. ERAI-LG
416 shows the strongest albedo contrast, which is twice as large compared to the experiment
417 with classic vegetation cover. These striking differences among the datasets mainly
418 drive the SNC results.

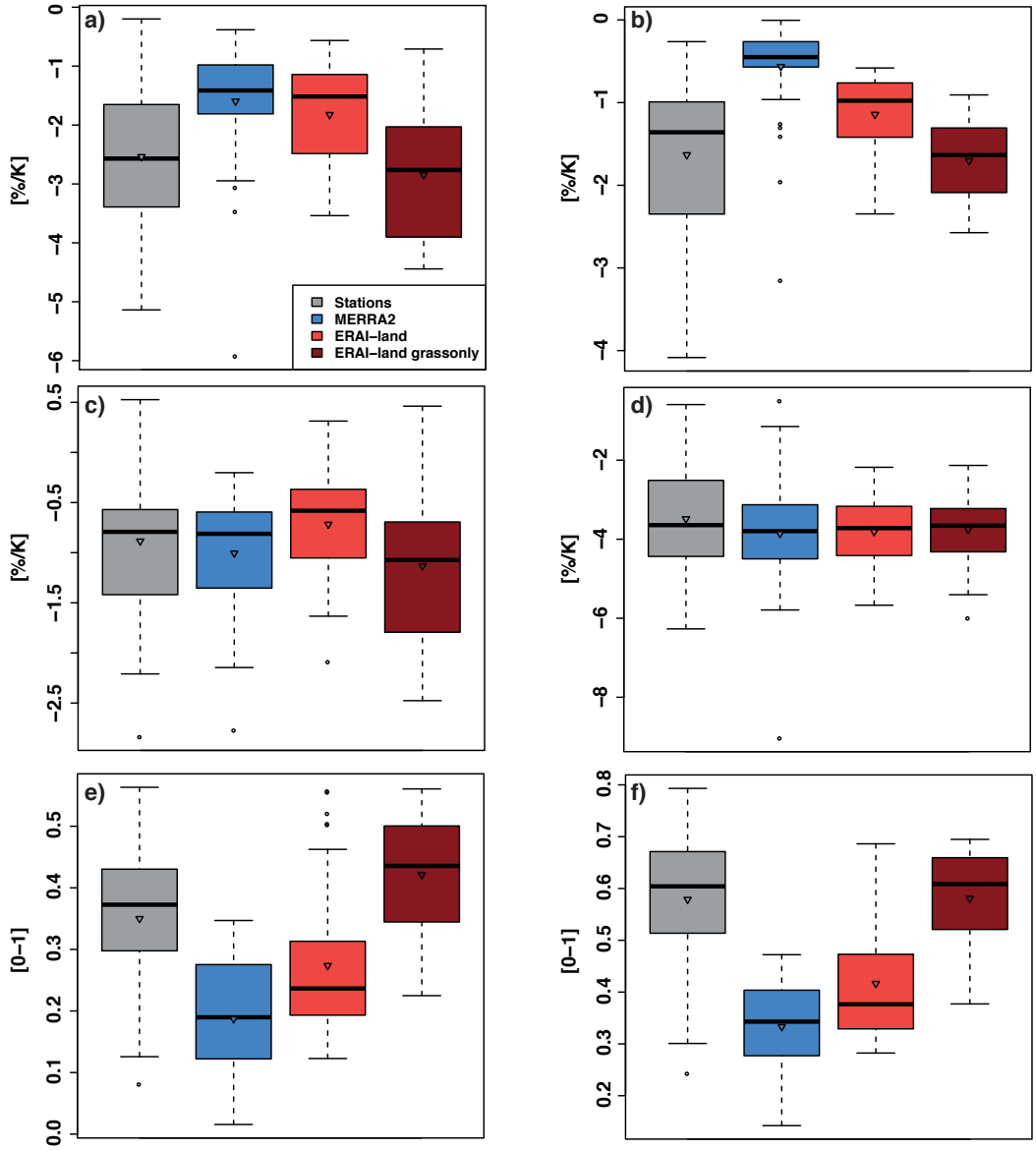

419

420 **Figure 4: Boxplot analysis for MAMJ 2000–2013 a) SNC+TEM, b) SNC, c) TEM,**
421 **d) snow melt sensitivity, e) albedo contrast and f) snow albedo. Triangle indicates**
422 **the mean value.**

423

424 Snow albedo is well captured by the grass-only experiment showing the same average
425 value around 0.6 as determined from the observations (Figure 4f). The standard
426 vegetation schemes used in MERRA2 and ERAI-L reduce the snow albedo in the
427 analyzed grid cells to 0.33 and 0.37. The differences in snow albedo between the
428 products is the main driver for the differences in the albedo contrast since the snow-

free albedo values are remarkably similar for all reanalysis products (Figure 5a). Nevertheless, they strongly deviate from the snow-free albedo determined from the observations, which is roughly twice as large compared to the reanalyses with a mean value of about 0.21 and which is very close to albedo values for grass (see e.g. **Betts and Ball 1997**, **Wei et al. 2001**).

To explore the impact of different factors on the TEM estimates, we show in Figure 5 mean values of temperature, snow cover and albedo, as well as the average change of snow albedo during spring. Also, to underline the crucial role of in-situ snow depth information, mean snow depth is shown. Mean station snow depth lies within the range of reanalyses values, with higher values reported by ERAI-LG. Moreover, stations have the lowest snow cover among all datasets (Figure 5 b and c). This difference is likely due to the conversion of snow depth to snow cover as well as from the precision (in centimeters) of the Russian snow depth measurement. Precision of snow depth diagnosed by reanalysis is much finer and the logarithmic conversion here can be performed more accurately. As a result, TEM values diagnosed by stations are probably too low. If we consider instead in-situ snow cover information from stations, the average snow cover is quite similar to reanalyses (ca. 55%), and the average TEM value gets stronger. However, replacing converted snow cover with observed snow cover in Eq. (2) is a questionable procedure, as the remaining terms were computed using snow depth conversion. Thus, for consistency we show lower values of TEM in Figure 4.

Temperature is well represented by all datasets with MERRA2 being about 1 K colder compared to stations, which is quite notable for such a robust varaiable. However, absolute values of temperature do not have a strong impact on the computation of TEM, since month-to-month changes in temperature affect both TEM and SNC computations. For ERAI-LG albedo contrast, the effect of the underestimated snow-free albedo and overestimated snow albedo cancel each other out. Finally, the snow albedo change during spring (Figure 5f) is very similar in station data and in MERRA2 (-0.09 average in both datasets), which points towards an adequate representation of snow metamorphosis and aerosol deposition in MERRA2. The ERAI-LG experiment shows a stronger change of snow albedo during spring than the standard version. ERAI-L potentially keeps the temperature and therefore snow metamorphosis more constant throughout spring due to a more stable local temperature climate induced by the

vegetaiton. Note also, that some stations show an increase of snow albedo during spring. This can be caused by fresh snow accumulation in late spring in some locations.

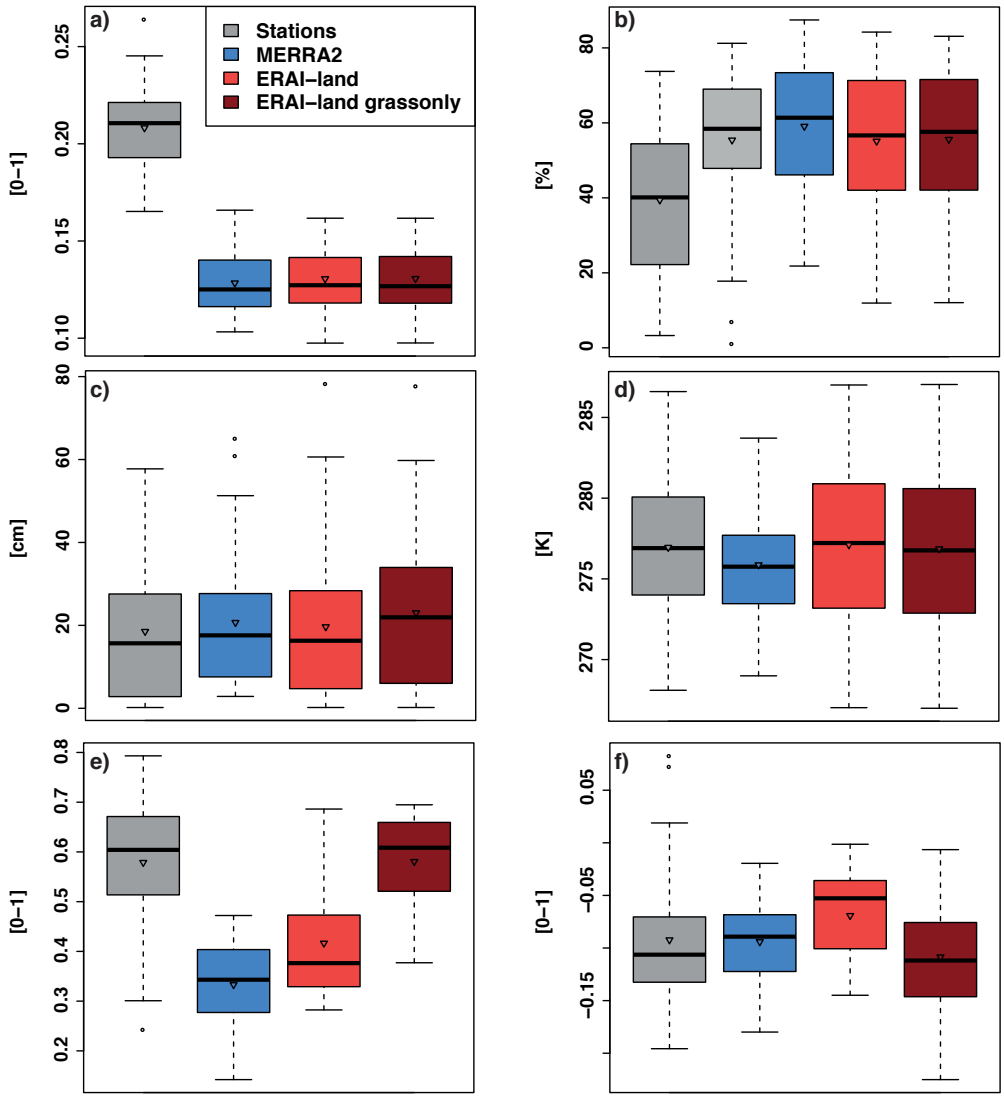

Figure 5: Boxplot analysis for MAMJ 2000–2013 a) snow free albedo, b) snow cover fraction, where the light grey boxplot is the originally observed snow cover from stations, c) snow depth, d) 2m temperature, e) mean albedo and f) snow albedo change within the season. Triangle indicates the mean value.

Figure 6 shows timeseries (2000–2013) for the mean values for SAF-related variables. Timeseries for SNC (Figure 6a) and TEM (Figure 6b) show that inter-annual variations of up to 0.5% K^{-1} are possible for both stations and reanalyses. Moreover, for both SNC and TEM, ERAI-LG seems to reproduce well the overall baseline and the magnitude of variability.

For snow melt sensitivity (Figure 6c) the agreement among the datasets is very good when it comes to magnitude and interannual variability, with MERRA2 showing an amplified inter-annual variability (up to 1.5% K^{-1}), which is beyond the magnitudes observed at stations. As already noted above, snow melt sensitivity seems to be a rather well reproduced process in modern reanalyses. Since snow-free albedo is quite constant over time in the reanalyses, the albedo contrast is dominated by the snow albedo (Figure 6d). ERAI-LG and the station network agree very well on the magnitude of snow albedo, whereas ERAI-L and MERRA2 fail to reproduce such high values. Magnitudes of inter-annual variability can reach up to ±0.05 in stations, with slightly weaker response in reanalyses. Correlation between stations and reanalyses is rather low, only individual years are captured correctly by ERAI-LG (see Supplement for correlation values).

Snow albedo change within spring (Figure 6e) is well captured by MERRA2 and ERAI-LG. Furthermore, ERAI-LG captures well the inter-annual varability for this metric. Specifically, variability during 2001–2004 and 2005–2008 periods is quite well represented. On the other hand, ERAI-L seems to lack the consistency with observations. Finally, as it was mentioned in section 4.1, snow depth variability (Figure 6f) is very well captured by all reanalyses. Again, ERAI-LG overestimates snow depth by up to 5 cm, with the other two reanalyses being on average 1-2 cm above the station values.

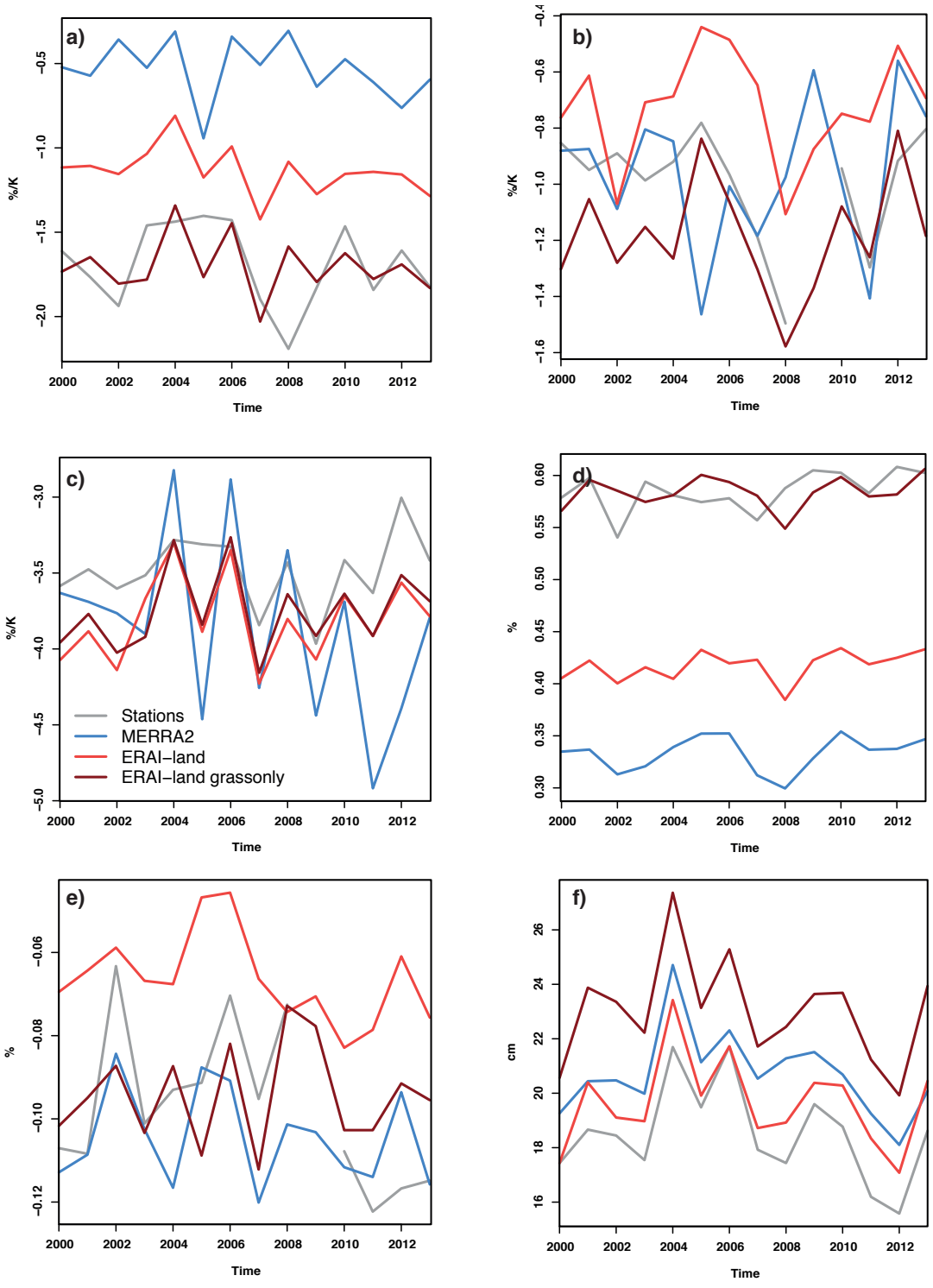

496

497 **Figure 6: Yearly timeseries of selected MAMJ SAF components averaged over all**
498 **44 locations. a) SNC, b) TEM, c) snow melt sensitivity, d) snow albedo, e) snow**
499 **albedo change within the season, f) snow depth.**

500

To further demonstrate the effect of the vegetation changes in the ERA-Interim land reanalysis, Figure 7 shows anomalies between ERAI-L and ERAI-LG. The structure follows Figure 6, with SNC and TEM shown in Figure 7a&b. As is clearly visible both variables are generally less negative in ERAI-L, a fact already known from timeseries and boxplot analysis. The largest impact of the vegetation changes is found for Northern Russia, the Pacific coast and the western region between Black and Caspian Sea. Interestingly, but as expected, snow melt sensitivity (Figure 6c) is not the key driver behind this distrubution. Since snow melt sensitivity is not directly linked to vegetation changes, the anomaly distribution is very heterogenous, with positive and negative anomalies over the whole domain. As known from the timeseries plot, snow sensitivity in ERAI-LG is overall slightly weaker than in ERAI-L, probably due to positive feedbacks such as reduction of nighttime cooling over higher vegetation types. The main driver behind the distribution of SNC is albedo contrast (Figure 7d). Albedo contrast is overall higher in ERAI-LG, especially along the borders of the domain, highlighted already for SNC.

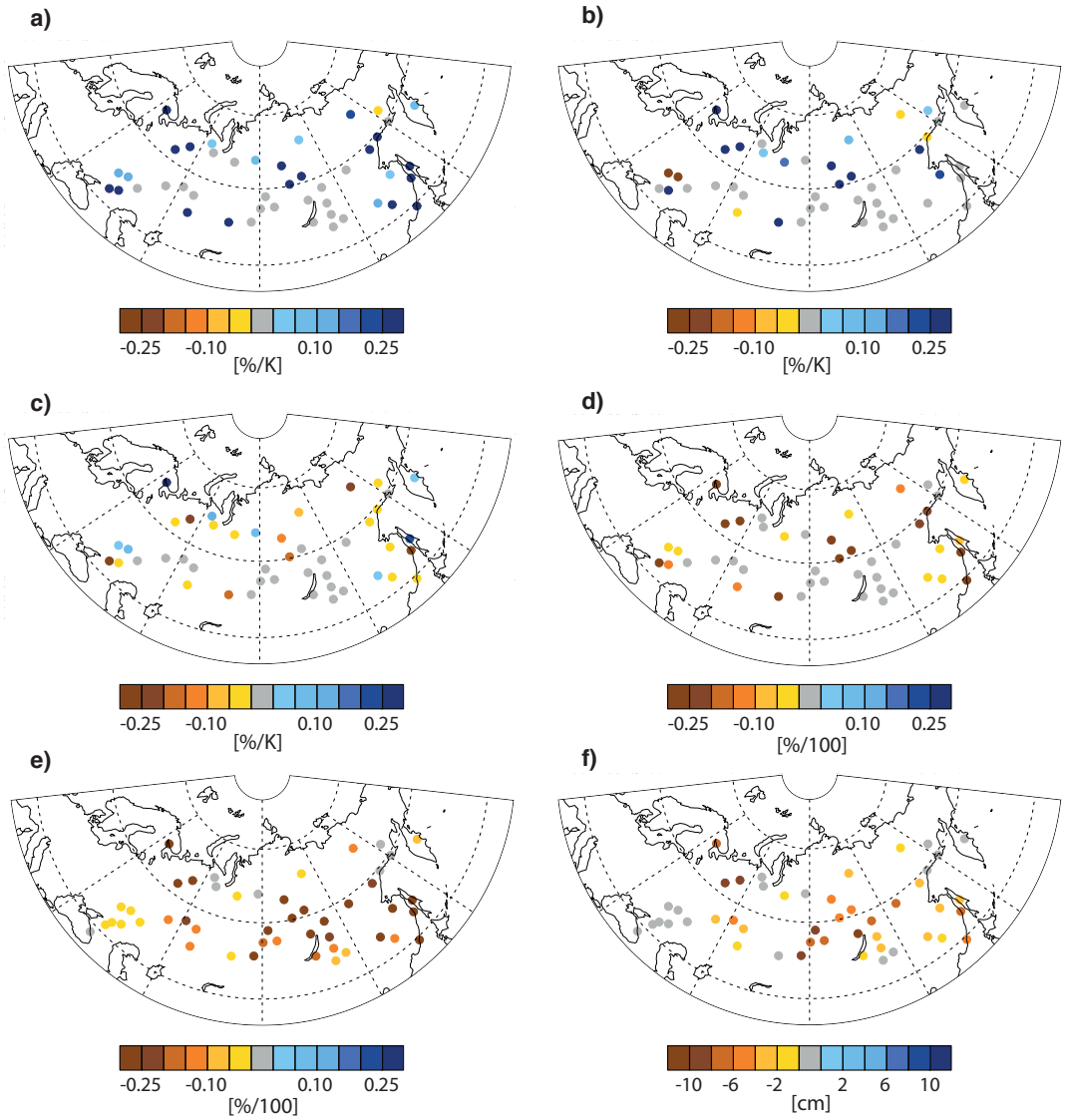

517

518 **Figure 7: Mean SAF components in anomalies of ERAI-L minus ERAI-LG for**
519 **2000-2013 MAMJ. a) SNC, b) TEM, c) snow melt sensitivity, d) mean albedo**
520 **contrast, e) mean albedo, f) snow depth.**

521

522

523 **5. Discussion**

524 We compared spring SAF and its components determined from in-situ measurements
525 over Russia for the period 2000–2013 with data derived from three modern reanalysis
526 products restricted to the grid cells including the observational sites. This was achieved
527 by using a unique collection of station measurements of radiation and snow

528 characteristics investigating for the first time observed SAF over this broad spatial and
529 temporal domain. Besides ERAI-L we also used a customized version of ERAI-L
530 (ERAI-LG), in which vegetation was set to grass in all concerned grid cells.

531 All three reanalysis datasets are completely independent from the analyzed station data.
532 While a direct comparison of point measurements with grid cell output always
533 introduces uncertainties due to the spatial varibailty of the surface, this is for now the
534 only way to evaluate reanalyses data using in-situ observations. An alternative option
535 would be satellite data, which come with their own uncertainties **(**e.g. **Romanov et al.**
536 **2002, Foster et al. 2005, Wang et al. 2014).**

537 Snow depth statistics derived from daily station data are reasonably well reproduced in
538 all three modern reanalyses, which is in agreement with **Wegmann et al. (2017)** who
539 investigated April snow depth in ERAI-L. While snow depth differences between
540 ERAI-L and ERAI-LG are small, ERAI-LG shows slightly higher deviations from the
541 station data than ERAI-L that might be caused by the higher vegetation in station
542 surroundings and by underestimation of snowfall due to instrumentation used at the
543 Russian station network (**Rasmussen et al. 2012**).

544 Day-to-day variability of albedo is notably higher in station data compared to any
545 reanalysis product. Besides spatial averaging over the reanalyses grid cells, this is
546 potentially caused by land surface changes due to weather (e.g. soil moisture change,
547 aerosol deposition), which are not represented in the reanalyses. However, ERAI-LG
548 demonstrates increasing albedo variability, nearly doubling the standard deviations
549 diagnosed by ERAI-L with the standard vegetation scheme.

550 The limitations of the station data imply some constraints for comparisons with
551 reanalysed data. As near-surface temperature is unavailable in station data, we used for
552 both stations and reanalyses 2m air temperature, which reduces the strength of the SAF
553 feedback. Moreover, using local 2m air temperature first and then average over our
554 domain later leads to lower SAF values than if we would have used NH averaged 2m
555 air temperature. Since albedo changes in our stations are much more dramatic (due to
556 the WMO conditions) than in model or satellite grid cells, using geographically
557 "smoothed" temperature data would eventually lead to a much stronger impact of
558 albedo changes on temperature changes. Thus, our results are not to be seen as a

559 Northern Hemisphere impact analysis but rather as a contribution to reanalysis
560 improvement and the investigation of SAF evolution.
561
562 Secondly, snow cover is underestimated in station data due to the measurement
563 precision of 1cm, which reduces the strength of the TEM component. The snow albedo
564 and the snow-free albedo are substantially higher in station data than in the reanalyses
565 with classic vegetation boundary conditions (MERRA2 and ERAI-L). Compared to
566 other observation-based studies, spring snow albedo and grass albedo derived from our
567 station network is quite realistic **(Roesch et al. 2009, Stroeve et al. 2006**). Thus, the
568 difference revealed by reanalyses is likely due to averaging over grid cells.

569 Results from ERAI-LG clearly demonstrate that SAF and its components are very close
570 to those in the station data. The largest improvement was found for albedo contrast and
571 for snow albedo, which both are more realistic in ERAI-LG. At the same time snow-
572 free albedo in all three reanalyses (including ERAI-LG) was found to be lower than in
573 the station data, because snow-free albedo in all reanalysis data sets is prescribed as a
574 monthly climatology from MODIS data. As MODIS mostly registers albedo from
575 Taiga and Tundra vegetation, a stark difference to the grass albedo from the stations
576 occurs.

577 MERRA2 shows the lowest SAF values resulting from a very low albedo contrast,
578 which is probably a consequence of the vegetation scheme in the MERRA2 land
579 module. On the other hand, MERRA2 represents TEM reasonably well most likely due
580 to the accurate representation of the intra-seasonal snow albedo changes. Thus, relative
581 snowpack changes appear to be well represented in MERRA2, probably also due to a
582 more accurate representation of aerosols.

583 In general, we found higher SAF values in ERAI-L than in the recent CMIP3/CMIP5
584 analyses of NH SAF by **Fletcher et al. (2015)**. This disagreement results from a variety
585 of factors. First, our domain is limited to Russia only, thus excluding considerable parts
586 of Eurasia as well as North America. In this respect our domain is set within a high
587 SAF region, which may explain higher SAF values compared to the NH average by
588 **Fletcher et al. (2015**). On the other hand, MERRA2 shows good agreements with the
589 NH CMIP4/5 SAF results, however mostly because the albedo contrast is very low.
590 Furthermore, as we pointed out above, in-situ observations used here tend to slightly

591 overestimate SAF, mainly due to higher snow albedo values. This is because in-situ
592 snow albedo is typically measured by a sensor installed over a vegetation-free snow
593 pack. The vegetation scheme used in reanalyses gives lower snow albedo values
594 implying realistic vegetation cover such as taiga or tundra. However, our MERRA2
595 results agree fairly well with the findings of **Fletcher et al. (2015)**. Moreover, mean
596 values of the albedo independent variable snow melt sensitivity are very close to the
597 "observational" snow melt sensitivity computed by **Fletcher et al. (2015).**

598 We also found agreements with **Fletcher et al. (2015)** in the representation of the
599 spatial pattern of the SAF components. **Fletcher et al. (2015)** as well as **Fernandes et**
600 **al. (2009)** have shown maxima in SAF over northern Canada, northern Siberia and
601 southwestern Eurasia. The relation of 60:40 between SNC and TEM, which is found in
602 modeled, satellite and reanalysis data, was replicated by our station network. We found
603 similar spatial patterns for SAF and its components in both stations and gridded data
604 specifically for Southern Russia, while the pattern of station responses is less
605 homogenous compared to the gridded data. Also consistent with **Fletcher et al. (2015)**,
606 we found higher snow melt sensitivity north of 50° N. Finally, albedo contrast
607 distribution, which closely follows the snow albedo pattern, is in very good agreement
608 with the gridded analysis of snow albedo by **Fletcher et al. (2015)**.

609 **6. Conclusions**

610 Reanalyses including land surface modules show a physically consistent representation
611 of SAF with realistic spatial patterns and area-averaged sensitivity estimates. ERAI-LG
612 shows a better performance in representing station-based estimates considering the
613 uncertainty associated with "point to grid cell" comparisons. Accounting for aerosol-
614 related processes would likely improve this performance in future reanalysis releases.
615 Thus, for the analysis and validation of large-scale temporal and spatial averages of
616 SAF modern reanalyses seem to be an appropriate tool.

617 However, for analysing processes on smaller scales and high temporal resolution
618 studies, a healthy dense station network is required. The idealized ERAI-LG simulation
619 also highlights the caveats of comparing in-situ observations with gridded model data.
620 In this study, we show these discrepancies in terms of albedo and snow depth. Other
621 variables, in particular 2m temperature, can be expected to have a similar signal arising
622 from the differences between the model's gridcell land cover and the actual station

conditions. Our findings show that the experimental approach in ERAI-LG allows for an enhanced use of in-situ observations to diagnose the SAF in not-forested areas.

Considering future studies, the extension to other regions and use of other regional in-situ data might give further insights into regional hotspots of SAF. Cross-validation efforts employing model, reanalysis, satellite and station data may help to generate blended products to investigate radiation and albedo feedbacks in the changing Arctic, a region where SAF is especially strong. Regional modelling, including a variety of multi-layer land surface models over areas with a relatively dense observation network can provide a quantitative estimation of uncertainties among complex variables such as snow depth, albedo or SAF.

Acknowledgements. This study was suported by the ARCTIC-ERA project funded by the Belmont Forum Fund through the ANR. OZ also benefited from the support by the Russian Ministry of Education and Science (project no. 14.613.21.0083, ID RFMEFI61317X0083). ED was supported by the Portuguese Science Foundation (FCT) under project IF/00817/2015.

654 **References**

655 Balsamo, G., Albergel, C., Beljaars, A., Boussetta, S., Brun, E., Cloke, H., Dee, D.,
656 Dutra, E., Muñoz-Sabater, J., Pappenberger, F., de Rosnay, P., Stockdale, T. &
657 Vitart, F. 2015: ERA-Interim/Land: a global land surface reanalysis data set.
658 Hydrology and Earth System Sciences, 19, 389-407

659 Betts, A. K., & Ball, J. H. 1997: Albedo over the boreal forest. Journal of Geophysical
660 Research: Atmospheres, 102, 28901-28909.

661 Bony, S., Colman, R., Kattsov, V.M., Allan, R.P., Bretherton, C.S., Dufresne, J., Hall,
662 A., Hallegatte, S., Holland, M.M., Ingram, W., Randall, D.A., Soden, B.J.,
663 Tselioudis, G. and Webb M.J. 2006: How Well Do We Understand and Evaluate
664 Climate Change Feedback Processes?. J. Climate, 19, 3445–3482

665 Brun, E., Vionnet, V., Boone, A., Decharme, B., Peings, Y., Valette, R., Karbou, F.,
666 and Morin, S 2013: Simulation of Northern Eurasian Local Snow Depth, Mass,
667 and Density Using a Detailed Snowpack Model and Meteorological Reanalyses, J.
668 Hydrometeorol., 14, 203–219

669 Brutel-Vuilmet, C., Ménégoz, M., & Krinner, G. 2013: An analysis of present and
670 future seasonal Northern Hemisphere land snow cover simulated by CMIP5
671 coupled climate models. The Cryosphere, 7, 67

672 Budkyo, M. I. 1967: The effect of solar radiation on the climate of the earth. Tellus,
673 21, 611-19

674 Bulygina, O. N., Groisman, P. Y., Razuvaev, V. N., & Radionov, V. F. 2010: Snow
675 cover basal ice layer changes over Northern Eurasia since 1966. Environmental
676 Research Letters, 5, 015004.

677 Cess, R. O., & Potter, G. L. 1991: Interpretation of snow-climate feedback as
678 produced by 17 general circulation models. Science, 253, 888

679 Cohen, J., Screen, J. A., Furtado, J. C., Barlow, M., Whittleston, D., Coumou, D.,
680 Francis, J., Dethloff, K., Entekhabi, D. & Overland J. 2014: Recent Arctic
681 amplification and extreme mid-latitude weather. Nat. Geosci., 7, 627–37

682 Collins, M., Knutti, R., Arblaster, J., Dufresne, J.-L., Fichefet, T., Friedlingstein, P.,
683 Gao, X., Gutowski, W.J., Johns, T., Krinner, G., Shongwe, M., Tebaldi, C.,
684 Weaver, A.J. & Wehner M. 2013: Long-term Climate Change: Projections,
685 Commitments and Irreversibility. In: Climate Change 2013: The Physical Science
686 Basis. Contribution of Working Group I to the Fifth Assessment Report of the
687 Intergovernmental Panel on Climate Change [Stocker, T.F., D. Qin, G.-K. Plattner,
688 M. Tignor, S.K. Allen, J. Boschung, A. Nauels, Y. Xia, V. Bex and P.M. Midgley
689 (eds.)]. Cambridge University Press, Cambridge, United Kingdom and New York,
690 NY, USA.

691 Curry, J. A., Schramm, J. L., Rossow, W. B., & Randall, D. 1996: Overview of Arctic
692 cloud and radiation characteristics. Journal of Climate, 9, 1731-1764.

693 Dee, D. P., Uppala, S. M., Simmons, A. J., Berrisford, P., Poli, P., Kobayashi, S.,
694 Andrae, U., Balmaseda, M. A., Balsamo, G., Bauer, P., Bechtold, P., Beljaars, A.
695 C. M., van de Berg, L., Bid- lot, J., Bormann, N., Delsol, C., Dragani, R., Fuentes,
696 M., Geer, A. J., Haimberger, L., Healy, S. B., Hersbach, H., Hólm, E. V., Isaksen,
697 L., Kållberg, P., Köhler, M., Matricardi, M., McNally, A. P., Monge-Sanz, B. M.,
698 Morcrette, J.-J., Park, B.-K., Peubey, C., de Rosnay, P., Tavolato, C., Thépaut, J.-
699 N., & Vitart, F. 2011: The ERA–interim reanalysis: Configuration and
700 performance of the data assimilation system, Q. J. Roy. Meteor. Soc., 137, 553–
701 597

702 Derksen, C. & R. Brown, 2012: Spring snow cover extent reductions in the 2008–
703 2012 period exceeding climate model projections. Geophysical Research Letters,
704 39.

705 Dufour, A., Zolina, O. and Gulev, S.K., 2016: Atmospheric moisture transport to the
706 Arctic: Assessment of reanalyses and analysis of transport components. Journal of
707 Climate, 29, 5061-5081.

708 Dutra, E., Balsamo, G., Viterbo, P., Miranda, P. M., Beljaars, A., Schär, C., & Elder,
709 K. 2010: An improved snow scheme for the ECMWF land surface model:
710 description and offline validation. Journal of Hydrometeorology, 11, 899-916.

711 Fernandes, R., H. Zhao, X. Wang, J. Key, X. Qu, & A. Hall 2009: Controls on

712 Northern Hemisphere snow albedo feedback quantified using satellite earth
713 observations, Geophys. Res. Lett., 36, L21702

714 Flanner, M. G., Shell, K. M., Barlage, M., Perovich, D. K., & Tschudi, M. A. 2011:
715 Radiative forcing and albedo feedback from the Northern Hemisphere cryosphere
716 between 1979 and 2008. Nature Geoscience, 4, 151.

717 Fletcher, C. G., Thackeray, C. W., & Burgers, T. M. 2015 Evaluating biases in
718 simulated snow albedo feedback in two generations of climate models. Journal of
719 Geophysical Research: Atmospheres, 120, 12-26.

720 Fletcher, C. G., Zhao, H., Kushner, P. J., & Fernandes, R. 2012: Using models and
721 satellite observations to evaluate the strength of snow albedo feedback. Journal of
722 Geophysical Research: Atmospheres, 117

723 Foster, J. L., Sun, C., Walker, J. P., Kelly, R., Chang, A., Dong, J., & Powell, H.
724 2005: Quantifying the uncertainty in passive microwave snow water equivalent
725 observations. Remote Sensing of environment, 94, 187-203

726 Gelaro, R., McCarty, W., Suárez, M.J., Todling, R., Molod, A., Takacs, L., Randles,
727 C.A., Darmenov, A., Bosilovich, M.G., Reichle, R., Wargan, K., Coy, L.,
728 Cullather, R., Draper, C., Akella, S., Buchard, V., Conaty, A., da Silva, A.M., Gu,
729 W., Kim, G., Koster, R., Lucchesi, R., Merkova, D., Nielsen, J.E., Partyka, G.,
730 Pawson, S., Putman, W., Rienecker, M., Schubert, S.D., Sienkiewicz, M. & Zhao
731 B. 2017: The Modern-Era Retrospective Analysis for Research and Applications,
732 Version 2 (MERRA-2). J. Climate, 30, 5419–5454

733 Graversen, R. G., & Wang, M. 2009: Polar amplification in a coupled climate model
734 with locked albedo. Climate Dynamics, 33, 629-643

735 Graversen, R. G., Langen, P. L., & Mauritsen, T. 2014: Polar amplification in
736 CCSM4: Contributions from the lapse rate and surface albedo feedbacks. Journal
737 of Climate, 27, 4433-4450.

738 Groisman, P. Y., Karl, T. R., Knight, R. W., & Stenchikov, G. L. 1994: Changes of
739 snow cover, temperature, and radiative heat balance over the Northern
740 Hemisphere. Journal of Climate, 7, 1633-1656.

741 Hall, A. 2004: The role of surface albedo feedback in climate. Journal of Climate, 17,
742 1550-1568.

743 Hall, A., & Qu, X. 2006: Using the current seasonal cycle to constrain snow albedo
744 feedback in future climate change. Geophysical Research Letters, 33(3).

745 Hall, A., Qu, X., & Neelin, J. D. 2008 Improving predictions of summer climate
746 change in the United States. Geophysical Research Letters, 35

747 Hirahara, S., Ishii, M., & Fukuda, Y. 2014: Centennial-scale sea surface temperature
748 analysis and its uncertainty. Journal of Climate, 27, 57-75.

749 Kanamitsu, M., Ebisuzaki, W., Woollen, J., Yang, S. K., Hnilo, J. J., Fiorino, M., &
750 Potter, G. L. 2002: Ncep–doe amip-ii reanalysis (r-2). Bulletin of the American
751 Meteorological Society, 83, 1631-1643.

752 Kevin, J. P. W., Kotlarski, S., Scherrer, S. C., & Schär, C. 2017: The Alpine snow-
753 albedo feedback in regional climate models. Climate Dynamics, 48, 1109-1124.

754 Kobayashi, S., Yukinari, O.T.A., Harada, Y., Ebita, A., Moriya, M., Onoda, H.,
755 Onogi, K., Kamahori, H., Kobayashi, C., Miyaoka, K. & Takahashi, K., 2015: The
756 JRA-55 reanalysis: General specifications and basic characteristics. Journal of the
757 Meteorological Society of Japan. Ser. II, 93, 5-48.

758 Lian, M. S., & Cess, R. D. 1977: Energy balance climate models: A reappraisal of
759 ice-albedo feedback. Journal of the Atmospheric Sciences, 34, 1058-1062.

760 Lindsay, R., Wensnahan, M., Schweiger, A., & Zhang, J. 2014: Evaluation of seven
761 different atmospheric reanalysis products in the Arctic. Journal of Climate, 27,
762 2588-2606.

763 Molod, A., Takacs, L., Suarez, M., & Bacmeister, J. 2015: Development of the
764 GEOS-5 atmospheric general circulation model: evolution from MERRA to
765 MERRA2. Geoscientific Model Development, 8, 1339-1356.

766 Pithan, F. & Mauritsen, T. 2014: Arctic amplification dominated by temperature
767 feedbacks in contemporary climate models. Nature Geoscience, 7,181.

768 Qu, X., & Hall, A. 2007: What controls the strength of snow-albedo feedback?.
769 Journal of Climate, 20, 3971-3981.

770 Qu, X., & Hall, A. 2014: On the persistent spread in snow-albedo feedback. Climate
771 dynamics, 42, 69-81

772 Rasmussen, R., Baker, B., Kochendorfer, J., Meyers, T., Landolt, S., Fischer, A.P.,
773 Black, J., Thériault, J.M., Kucera, P., Gochis, D., Smith, C., Nitu, R., Hall, M.,
774 Ikeda, K., & Gutmann E. 2012: How Well Are We Measuring Snow: The
775 NOAA/FAA/NCAR Winter Precipitation Test Bed. Bull. Amer. Meteor. Soc., 93,
776 811–829

777 Reichle, R. H., Draper, C. S., Liu, Q., Girotto, M., Mahanama, S. P., Koster, R. D., &
778 De Lannoy, G. J. 2017: Assessment of MERRA-2 land surface hydrology
779 estimates. Journal of Climate, 30, 2937-2960.

780 Rienecker, M.M., Suarez, M.J., Gelaro, R., Todling, R., Bacmeister, J., Liu, E.,
781 Bosilovich, M.G., Schubert, S.D., Takacs, L., Kim, G., Bloom, S., Chen, J.,
782 Collins, D., Conaty, A., da Silva, A., Gu, W., Joiner, J., Koster, R.D., Lucchesi, R.,
783 Molod, A., Owens, T., Pawson, S., Pegion, P., Redder, C.R., Reichle, R.,
784 Robertson, F.R., Ruddick, A.G., Sienkiewicz, M. & Woollen, J. 2011: MERRA:
785 NASA's Modern-Era Retrospective Analysis for Research and Applications. J.
786 Climate, 24, 3624–3648

787 Robock, A. 1983: Ice and snow feedbacks and the latitudinal and seasonal distribution
788 of climate sensitivity. Journal of the Atmospheric Sciences, 40, 986-997.

789 Roesch, A., Gilgen, H., Wild, M., & Ohmura, A. 1999: Assessment of GCM simulated
790 snow albedo using direct observations. Climate dynamics, 15, 405-418.

791 Romanov, P., Gutman, G., & Csiszar, I. 2002: Satellite-derived snow cover maps for
792 North America: accuracy assessment. Advances in space Research, 30, 2455-2460.

793 Schiffer, R. A., & Rossow, W. B. 1983 The International Satellite Cloud Climatology
794 Project(ISCCP)- The first project of the World Climate Research Programme.
795 American Meteorological Society, Bulletin, 64, 779-784.

796 Schneider, S. H., & Dickinson, R. E. 1974: Climate modeling. Reviews of

797 Geophysics, 12, 447-493.

798 Serreze, M. C., & Barry, R. G. 2011: Processes and impacts of Arctic amplification:
799 A research synthesis. Global and Planetary Change, 77, 85-96.

800 Stroeve, J. C., Box, J. E., & Haran, T. 2006: Evaluation of the MODIS (MOD10A1)
801 daily snow albedo product over the Greenland ice sheet. Remote Sensing of
802 Environment, 105, 155-171.

803 Thackeray, C. W., & Fletcher, C. G. 2016: Snow albedo feedback: Current
804 knowledge, importance, outstanding issues and future directions. Progress in
805 Physical Geography, 40, 392-408.

806 Wang, Z., Schaaf, C.B., Strahler, A.H., Chopping, M.J., Román, M.O., Shuai, Y.,
807 Woodcock, C.E., Hollinger, D.Y. & Fitzjarrald, D.R. 2014: Evaluation of MODIS
808 albedo product (MCD43A) over grassland, agriculture and forest surface types
809 during dormant and snow-covered periods. Remote Sensing of Environment, 140,
810 60-77.

811 Wei, X., Hahmann, A. N., Dickinson, R. E., Yang, Z. L., Zeng, X., Schaudt, K. J.,
812 Schaaf, C.B. & Strugnell, N. 2001: Comparison of albedos computed by land
813 surface models and evaluation against remotely sensed data. Journal of
814 Geophysical Research: Atmospheres, 106, 20687-20702.

815 Wegmann, M., Orsolini, Y., Dutra, E., Bulygina, O., Sterin, A., & Brönnimann, S.
816 2017: Eurasian snow depth in long-term climate reanalyses. The Cryosphere, 11,
817 923.

818 Wexler, H. 1953: Radiation balance of the Earth as a factor in climatic change. In:
819 Shapley H (ed) Climatic Change. Cambridge: Harvard University Press,73-105

820 Xiao, L., Che, T., Chen, L., Xie, H., & Dai, L. 2017: Quantifying Snow Albedo
821 Radiative Forcing and Its Feedback during 2003–2016. Remote Sensing, 9, 883.

822